

TEKNOFEST İSTANBUL
AEROSPACE AND TEKNOLOGY FESTIVAL
FIGTHING UAV COMPETITION
CRITICAL DESIGN REPORT

TEAM NAME: ALYA

**WRITERS: Ahmet OĞURTAN, Faruk ÇORUM, Melih ÇİMEN,
Ahmed JABER, Çağatay BÜTÜN, Duygu KAYTAN**



Table of Contents

1. FUNDEMENTAL SYSTEM SUMMARY	3
1.1. System Definition	3
1.2. System Performance Properties	4
2. Organization Summary	4
2.1. Team Organization.....	4
2.2. Time Flowchart and Budget.....	5
2.3. Final System Architecture.....	6
2.4. Subsystem Summary.....	10
2.5. Aircraft Performance Report.....	12
3.4 3D Design of UAV	15
3. Autonomous Lockdown.....	18
4. Communication.....	22
5. User Interface Design.....	26
6. AIRCRAFT INTEGRATION	28
6.1. Structural Integration	28
6.2. Mechanical Integration	29
6.3. Electronic Integrationn.....	31
7. TEST VE SIMULATION	31
7.1. Subsystem Tests	31
7.2. Flight Test and Control List	38
8. Safety	39
9. REFERENCES	40

1. FUNDEMENTAL SYSTEM SUMMARY

1.1. System Definition

The system is an unmanned aerial vehicle (UAV) that can fly autonomously. Its mission is to perform dog-fight with other aircraft autonomously. It is specially designed to have superior maneuverability capabilities and high speed during combat to be in an advantageous situation in battle.

The UAV system consists of the following sub-systems:

- Ground control station
 - Laptop (computer)
 - Telemetry receiver
 - Radio transmitter
- Aircraft
 - Thrust System
 - Radio controlled motors
 - Electronic speed controllers
 - Propellers
 - Communication system
 - Telemetry transmitter
 - Radio receiver
 - Image Processing system
 - Raspberry Pi 4
 - Camera module of the Raspberry Pi 4
 - Wide angle lens of the camera module
 - Autonomous flight system
 - Pixhawk flight controller
 - Buzzer
 - fuse
 - GPS sensor
 - Maneuver system
 - Servo motors
 - Control surfaces (ailerons, elevator, rudder)
 - Power Supply System
 - Battery
 - PDB
 - Switch

The ground control station consists of a laptop computer that is connected to a telemetry receiver, and a separate radio transmitter. The telemetry receiver takes the telemetry data from the telemetry transmitter, which is located in the aircraft, and sends it to the computer so that the operator of the ground control station can see the camera view. In addition, the operator can interfere with the aircraft if necessary. The radio transmitter can be used to manually control the aircraft if necessary.

The “Rüzgar” UAV is designed to have superior capabilities in air to air combat with other aircraft. Propulsion system, which consists of the electrically powered propeller, and the control surfaces are selected and sized to provide superior maneuverability. The UAV is equipped with a communication system, image processing system, and automatic flight control system. Communications system enables the aircraft to communicate with the ground station; image processing system enables detection of another aircraft, and the automatic flight control system enables the autonomous flight.

1.2. System Performance Characteristics

Table 1.1 Performance Properties of the “Rüzgar” UAV

Endurance (Flight time), hours	1/2
Cruise speed, m/s	20
Maximum speed, m/s	30
Stall speed, m/s	8.67
Takeoff speed, m/s	11.5
Telemetry transfer speed, Mbps	1.0
Maximum altitude, km	<5
Range, km	<1
Telemetry transfer range, km	5
Drag polar	$C_D = 0.083 + 0.07C_L^2$
K	0,07

Table 1 shows that the cruise speed and the maximum speed of the aircraft are increased compared to the values indicated in the pre-design report. In the pre-design report, the cruise speed was 15 m/s but, it is 20 m/s now. This improvement has been made after reviewing the RC airplane dogfights, where the airplanes are unable to catch enemy planes because they are not responding quickly enough. The UAV has a conventional configuration consisting of a fuselage, a wing, and a tail, equipped with the control surfaces.

2. Organization Summary

2.1. Team Organization

The organization diagram of the team is shown in Fig. 1. The team is organized such that 3 major tasks, which are hardware, software, and electronics, are targeted by the designated team members. The hardware task includes the design and selection of the necessary subsystems, and manufacturing the structure of the airplane. The software task includes algorithm development for the object detection and tracking; the code must be compatible with the Ardupilot code. In addition, the interface with the ground station must be established. The electronics task includes selection of the telemetry and radio connections to provide the communication with the ground station during the mission. The advisors' duty is to provide support and supervision during the design process.

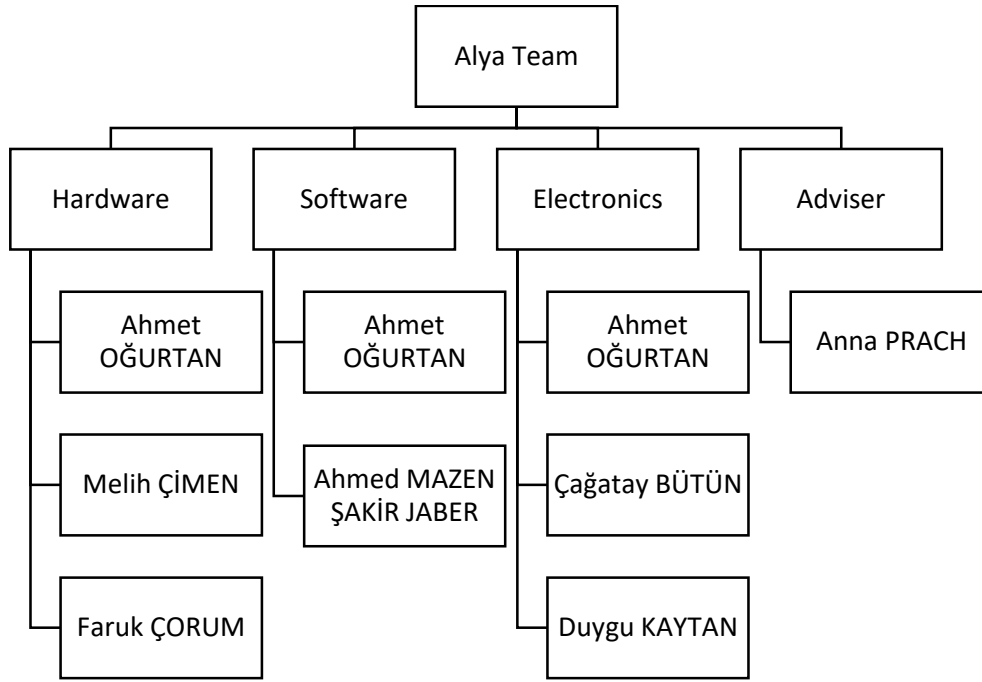


Figure 2.1 Team Organizational Scheme

2.2. Time Flowchart and Budget

The time flowchart for the project that is presented in the pre-design report as well teams current standing in the timeline can be seen in the Fig. 2.2.



Figure 2.2 Time Flow Chart Comparison and the Team's Current Standing

Figure 2.2 illustrates the planning of the project. The hardware design has been completed. The software design and manufacturing are in the progress. Several delays in the software design and manufacturing are caused by the problems with the compatibility between the simulation environment, operating system, and the deep learning algorithm, as well as modifications in the UAV configuration.

An approximate budget estimation is shown in Table 2.1. Several adjustments are made as compared to the budget estimation made in the pre-design report. These adjustments are done considering the current market prices of the parts, and the budget increase occurs due to the increased inflation rates in Turkey in the past several months.

Table 2.1 Approximated Budget

Material	Total price in pre-design Report [₺]	Total price in conceptual design report [₺]
Electrical Motor	623.7	784,48
Servo Motor	209.4	527.04
Electronic Speed Controller (ESC)	512.1	646,55
Telemetry receiver	320,66	360
Telemetry transmitter	289,90	303.84
Battery	1082.64	2520
Camera	1.057,12	1.159,51
Camera lens	493,32	541,11
Image processing Computer	863,32	946,94 TL
Geographic position sensor (GPS)	736.96	793.28
Flight Controller	2.018,72	3023.84
Balsa Wood [2-3 cm]	600,00	750,00
Insulation foam [5-8 cm]	750,00	-
Small wheel	90,00	-
Duct tape	60,00	-
Radio transmitter/receiver	2.688,15	3.529,01
Propeller	310.43	120,69
Fuse electronic	5,29	132,23
Power Distribution Board (PDB)	-	682.5
	12311.71 [₺]	15874,08 [₺]

The manufacturing methods have been modified. In order to increase the rigidity of the wing, instead of using insulation foam it has been decided to use balsa and spar as the inner material of the wing, and carbon fiber for the outer part of the wing. This modifications do not effect the budget since the cost of the new structural materials is not essential compared to the cost of the electronic components.

2.3. Final System Architecture

The final system architecture consists of the main elements shown in Fig. 3.1. The first major element is the aircraft, and the second is the ground station. The general operating principle is that the aircraft is controlled by the ground station via an interface, and

communicates through the telemetry. The detailed descriptions of the subsystems and the communications are presented further in the report. Table 3.1 provides the list of the components.

Figure 3.1 Final System Architecture

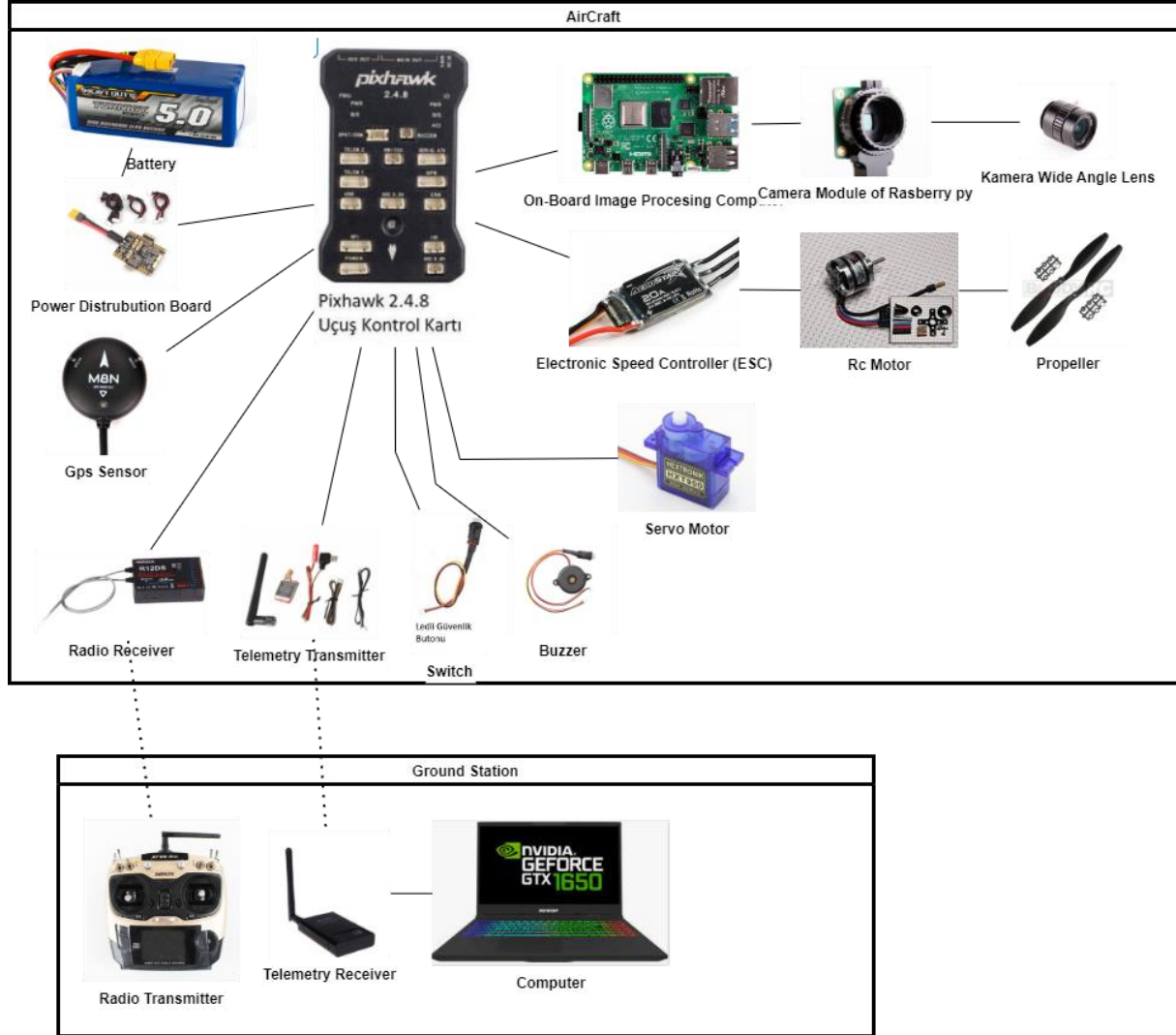



Table 3.1 System Components

List of Components




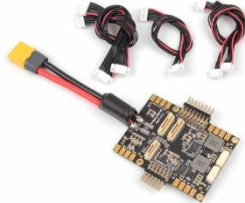
Number	Model	Picture
1	Raspberry Pi 4 2GB	

SAVAŞAN İHA YARIŞMASI 2021

2	Raspberry Pi HQ Camera	
3	6mm Wide Angle Lens of Raspberry Pi HQ Camera	
4	Pixhawk 2.4.8 Flight Control Set	 Pixhawk 2.4.8 Uçuş Kontrol Kartı
5	Radiolink AT9SG Pro 10 Channel 2.4GHz	
6	R12DS Radio Receiver Set	
7	Telemetry Transmitter 5.8 GHz 600mW FPV Transmitter	

SAVAŞAN İHA YARIŞMASI 2021

8	Telemetry receiver 5.8 GHz 8 Channel RC805 FPV Receiver Module	
9	Monster Abra A5 V15.1 15,6"	
10	FMS 850KV 3536 OUTRUNNER	
11	SKYWALKER-50A-UBEC-5A	
12	11x7 Propeller APC brand	
13	HXT900 Micro Servo 1.6kg / 0.12sec / 9.8g	
14	Holybro M8N GPS	

15	RUDDOG 5000mAh 50C 14.8V LiPo Stick Pack Battery with XT90 Plug	
16	PX4 Pixhawk Buzzer [2.4.6/2.4.8]	
17	PX4 Pixhawk Switch	 Ledli Güvenlik Butonu
18	Pixhawk 4 Power Module (PM07) (PDB)	
		6

2.4. Subsystem Summary

Image Processing Subsystem:

Image processing system's goal is to gather visual data and process it. For that it needs the following items:

- Raspberry Pi 4 2GB
- Raspberry Pi HQ camera
- Raspberry Pi HQ camera 6mm wide angle lens

The computer receives the video stream from the camera, processes it, and send it to the flight controller as well as the ground station via telemetry transmitter. Raspberry Pi 4 with 2 GB RAM is selected as an image processing computer since it's performance characteristics are sufficient for the particular application, in particular receiving and processing the image data. The camera, that has been chosen, is the camera of the Raspberry Pi so they are compatible with each other. The entire system is powered by a lithium battery.

Autonomous Flight System:

This system's goal is to make the aircraft fly autonomously. It consists of the following parts:

- Pixhawk 2.4.8 flight controller

- PX4 Pixhawk buzzer
- Switch
- Holybro M8N GPS

The flight controller is the heart of the autonomous flight since it sends the necessary data to RC motors and the servo motors that actuate the control surfaces. Three alternative flight controllers are analyzed, including the Pixhawk, Arducopter, and ArduPilot. As a result, the Pixhawk is selected as the best option for the design. The buzzer provides the altitude values to the flight controller via sound waves; the Pixhawk's buzzer has been chosen so that the flight controller and the buzzer would be compatible. The flight controller requires the geographic data, therefore a GPS is needed. The chosen GPS is Holybro M8N GPS, which is compatible with the Pixhawk, and provides the desired precision. The Switch is the key that opens and closes Pixhawk is a security measure, and comes with the Pixhawk package.

Communication System

The communication system's goal is to handle transfer of the data between the ground station and the aircraft. It consists of the following components:

- 5.8 GHz 8 Channel RC805 FPV receiver module
- 5.8 GHz 600Mw FPV transmitter
- Radiolink AT9SG Pro 10 channel 2.4Ghz
- R12DS radio receiver set
- Monster Abra A5-V15.5 (computer)

The telemetry receiver and transmitter must be compatible with each other, and use the same frequency channel to communicate and transfer the necessary data. They do not need to be compatible with the radio receiver and the transmitter. In this regard, and also by considering the communication rule book that is given by Teknofest, these pair of telemetry components have been chosen as shown in Table 3.2.

Table 3.2 Telemetry Components

Telemetry Transmitter 5.8 GHz 600Mw FPV Transmitter
Telemetry receiver 5.8 GHz 8 Channel RC805 FPV Receiver Module

The radio communication is necessary for manual flight while telemetry data is only necessary for the users to comprehend and verify the situation of the aircraft, the response of the aircraft to detected enemy aircraft, as well as the misdetection and other system parameters. The radio communication components must operate at the same frequency, and must be compatible with each other. It is important to note that the frequency value of the radio transfer and the frequency value of telemetry transfer should not be the same since interference may occur and corrupt the data. The radio communication components selected for the design are given in Table. 3.3.

Table 3.3 Radio Communication Components

Radiolink AT9SG Pro 10 Channel 2.4Ghz
R12DS Radio Receiver Set

Power Supply System

This system's goal is to supply the necessary amount of power to every component of the aircraft. The following components are included:

- RUDDOG 5000mAh 50C 14.8V LiPo Stick Pack Battery with XT90 Plug
- Pixhawk 4 Power Module (PM07)

A LiPo battery is chosen since it has a high specific energy density, and is safe in use. The battery is chosen such that it provides sufficient power for the UAV to complete one round in the competition. The power distribution board is selected so that each component in the system can get the required current. In addition, the power distribution board must be compatible with the Pixhawk4.

Thrust (Propulsion) System

This system's goal is to provide the necessary amount of thrust so that the aircraft can fly. The following components are included:

- FMS 850KV 3536 OUTRUNNER
- SKYWALKER-50A-UBEC-5A
- 11x7 Propeller APC brand

The propulsion system must provide sufficient thrust to overcome the aerodynamic drag of the aircraft. The engine is selected after the estimation of the drag of the aircraft. The propellers are the RC engine 11X7 propellers, with the diameter of 11 inches, and pitch angle equal to 7 deg. Electronic speed controllers are selected according to the maximum current requirement of the 50 Amp motor.

Maneuver System

This system's goal is to provide desired maneuverability characteristics of an aircraft. It includes

- Control surfaces (ailerons, elevator, rudder??? which ones???)
- Servo motors

The servo motors drive (rotate) the control surfaces of the aircraft. The control surfaces' deflections generate the moments that cause rotational motion. Servos are selected considering the magnitudes of the moments and the sizes of the control surfaces. HXT900 Micro Servo 1.6 kg is chosen it can apply moment up to 1.6 kg-cm

2.5. Aircraft Performance Analysis

Performance analysis is done to verify that the “Rüzgar” UAV is able to complete the round in the competition. First, the aerodynamic drag of the aircraft is estimated. The power required is equal to the drag multiplied by the airspeed. Next, the energy requirements are estimated from the power required and the flight time.

The subsonic parasite drag is estimated by using the component buildup method which estimates the drag contribution of each part of the aircraft. The following equations are referenced from [6].

$$(C_{D0})_{subsonic} = \frac{\sum(C_{fc}^{FF} Q_c S_{wet,c})}{S_{ref}} + C_{D,misc} + C_{D,LP}. \quad (1)$$

The mass-geometry characteristics of the airplane are given in Table 3.4.

Table 3.4 Mass and Geometry Characteristics

Roor Chord [m]	0,490
Tip Chord [m]	0,196
Mean Chord [m]	0,364
Span [m]	1,714
Surface Area [m^2]	0,587
Weigth [N]	28,812
Mass [kg]	2,937
Aspect Ratio	5

The values of the wetted areas of parts of the aircraft, which are required for the drag estimation are given in Table 3.5.

Table 3.5 Wetted areas

Total wetted area / wing area [-]	3,14
Total wetted area [m^2]	1,84
Wetted wing area [m^2]	1,17
Wetted tail area [m^2]	0,66
Wetted fuselaj area [m^2]	0.0012

Flat plate skin coefficients are estimated using the following equations.

$$C_{filamimar} = \frac{1.328}{\sqrt{Re}} \quad (2)$$

$$C_{f,turbulent} = \frac{0.455}{(\log(Re))^{0.28} (1 + 0.144M^2)^{0.65}} \quad (3)$$

Form factor for wing and tail are estimated from

$$FF = \left[1 + \frac{0.6}{\left(\frac{x}{c}\right)_m} \left(\frac{t}{c}\right) + 100 \left(\frac{t}{c}\right)^4 \right]. \quad (4)$$

And the Hinged surfaces have %10 more form factors, yielding

$$FF_{wing,tail} = 1.1FF \quad (5)$$

The form factor for the fuselage is calculated from

$$FF = (1 + \left(\frac{60}{f^3}\right) + \frac{f}{100}), \quad (6)$$

where

$$f = \frac{l}{d} = \frac{l}{\sqrt{\frac{4}{\pi} A_{max}}} \quad (7)$$

The component interference factor Q are constant values, and given in Table 3.6

Table 3.6 Interference Factor Values

Wing [-]	1
Horizontal tail [-]	1.08
Vertical tail [-]	1.08
Fuselage [-]	1

The miscellaneous drag due to antenna and other parts are assumed %10 of the total drag and thus the following equation,

$$C_{D,misc} = 0.1C_{D0,basic}. \quad (8)$$

Leakages and the profile turbulence drag are also assumed to be %10 of the total drag and thus the following equation,

$$C_{D,L\&P} = 0.1C_{D0,basic}. \quad (9)$$

With all this, it can finally calculate the parasitic drag of the aircraft.

Table 3.7 Components Drag Coefficients

Coefficient drag of wing	2,52E-02
Coefficient drag of tail	2,42E-02
Coefficient drag of fuselage	2,00E-02

The total zero-lift drag coefficient is obtained as the sum of the drag coefficients of the individual parts, and is equal to 0.07. Using Eqns. (7) and (8), the parasite drag coefficient is calculated to be equal to 0.083.

The total drag coefficient is given by

$$C_{D_{Total}} = C_{D_0} + C_{D_i}, \quad (9)$$

where $C_{D_i} = kC_l^2$ represents the induced drag, and

$$k = \frac{1}{\pi A R e} \quad (10)$$

Note that the 'e' is the Oswald's efficiency ratio which for delta wings is equal to,

$$e = 1.78(1 - 0.045AR^{0.68}) - 64 \quad (11)$$

From Eqn.(10), (11), parameter $e = 0.91$. It should be noted that these equations are estimates, not exact values, and in the real world, the value of Oswald's efficiency factor should be around 0.7-0.8 for the wing configuration. As a result, $k = 0.07$. The induced drag coefficient is calculated from

$$C_{D_i} = kC_l^2. \quad (12)$$

The total drag of the aircraft is given by the drag polar equation,

$$C_{D_{Total}} = 0,083 + 0,07C_l^2 \quad (13)$$

The total aerodynamic drag of the airplane is obtained from

$$D = \frac{1}{2} C_D S \rho V^2. \quad (14)$$

Since both lift and drag are the functions of the aircraft airspeed, the values of the aircraft drag at the minimum and maximum airspeeds are given in Table 3.7.

The table 3.7 Aircraft Drag Estimates

Drag at Min speed [N]	5,58
Drag at max speed [N]	24,60

The power required is found from Eqn. (15), yielding the value of 720 Watts when flying at the maximum speed.

$$P = T v \quad (15)$$

In cruise flight, the airspeed is equal to 20 m/s, resulting in the aerodynamic drag of 12.5 N. It is assumed that Rüzgar will be flying at the cruise speed in 80% of the competition, at maximum speed in 10%, and at minimum speed in the remaining 10%. As a result of these assumptions, the required total energy is calculated to be equal to 69.845 J.

3.4 3D Design

The 3D drawing of the UAV is done using the Autodesk Inventor Professional program, and is shown in Fig. 3.2. The subsystems that will be used are drawn according to their placements in the fuselage as shown in Fig. 3.3

Figure 3.2 3D Design of Rüzgar Aircraft

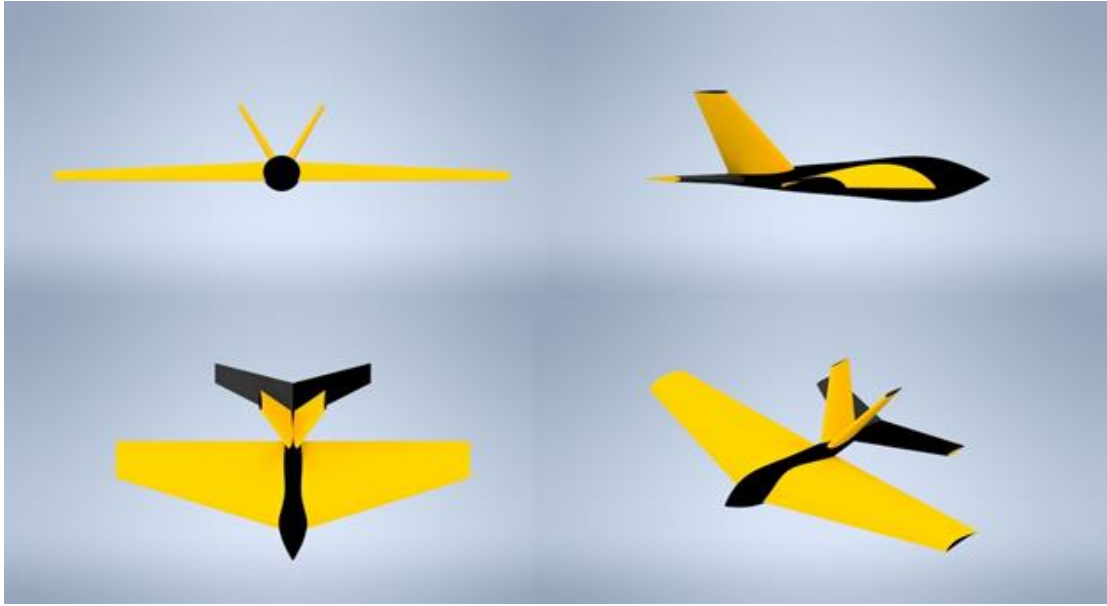
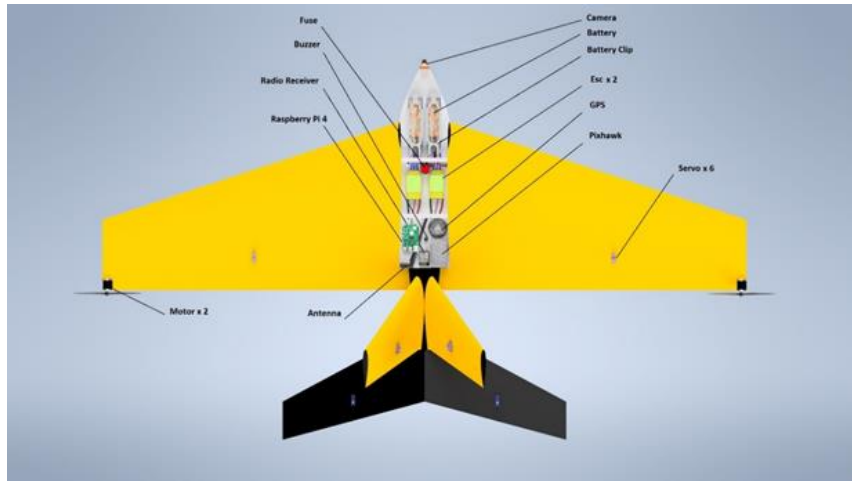


Figure 3.3 Locations of the Components



In the 3D design, the hardware systems are positioned on the UAV. Due to the importance of the center of gravity, heavy parts such as the battery are positioned at the very front of the body. Therefore, the center of gravity is in front of the aerodynamic center, thus providing the positive static margin, and therefore static stability. It is planned to place the all subsystems in the fuselage by fixing them with tape and screws in order to prevent disturb the stability of the UAV by moving during the flight and not to endanger the flight. In this way, the UAV can fly safely in sudden maneuvers. The specification of the UAV is shown in Table 3.8, including general specifications, performance characteristics, main wing and tail characteristics.

Table 3.8 Specification of the Rüzgar UAV

General Specifications	Performance	Main Wing	V Tail	Horizontal Tail
------------------------	-------------	-----------	--------	-----------------

Length	1.073 m	Max Speed	35.7 m/s	Airfoil	FX74-Cl5-140 MOD smoothed	NACA 0016	NACA 0016
Take Off Weight	3.5 kg	Cruise Speed	25 m/s	Wingspan	1.7 m	0.6 m	0.8 m
Range	<1 km	Stall Speed	9.87 m/s	Area	0.595 m ²	0.1 m ²	0.13 m ²
Endurance	30 min	Wing Loading	5.042 kg/m ²	Root Chord	0.5 m	0.215 m	0.215 m
Fuselage Diameter	0.15 m	Engine Power	800 W	Tip Chord	0.2 m	0.108 m	0.108 m
		Climb Rate	57°	Aspect Ratio	4.857	3.72	4.95
				Taper Ratio	0.4	0.5	0.5
				Tip chord offset	0.3 m	0.215 m	0.215 m

3.5 Weight Distribution of UAV

The location of the center of gravity of the UAV is determined from the weights of the individual components, and their corresponding locations, as shown in Table 3.8, and Fig. 3.4. The center of gravity of the UAV is 22.3 cm behind the wing tip according to the XFLR5 program. As a result of the calculations, it was found that the center of gravity should be 10.2 cm behind the wing tip for the UAV to fly properly and be stable. Therefore, weight was added to the tip of the fuselage cone and corrected so that the center of gravity was 10.2 cm behind the wing tip.

Table 3.9 Weight Characteristics and C.G. Location

	Weight [g]	X(CoG) [m]	Y(CoG) [m]	Z(CoG) [m]
Fuselage(empty)	300	0.199	0	0
Battery	490	-0.075	0.024	0.018
Battery	490	-0.075	-0.024	0.018
Battery Clip	40	-0.075	0.024	0.02
Battery Clip 2	40	-0.075	-0.024	0.02
Engine 1	245	0.5	0.850	-0.02115
Engine 2	245	0.5	-0.850	-0.02115
Propeller	23	0.5	0.850	-0.02115

SAVAŞAN İHA YARIŞMASI 2021

Propeller	23	0.5	-0.850	-0.02115
Wing	500	0.1621	0	0
Servo 1	10	0.3	0.425	-0.012
Servo 2	10	0.3	-0.425	-0.012
Elevator	250	0.7207	0	0
Servo 1	10	0.775	0.2	-0.0215
Servo 2	10	0.775	-0.2	-0.0215
Fin	200	0.5707	0	0
Servo 1	10	0.625	0.1	0.140
Servo 2	10	0.625	-0.1	0.140
Esc	35	0.035	0.0012	0.0062
Esc	35	0.035	-0.0012	0.0062
Raspberry pi 4	46	0.185	-0.028	0.0005
Pixhawk	15.8	0.264	0	0.0006
GPS	32	0.4	0.23	0.001
Camera	3	-0.15	0	0
Radio Receiver	14	0.45	0	0
Antenna	15	0.45	-0.1	0
Fuse	5	0	0	0.118
Buzzer	7	0.44	-0.02	0

Center of
Gravity of UAV

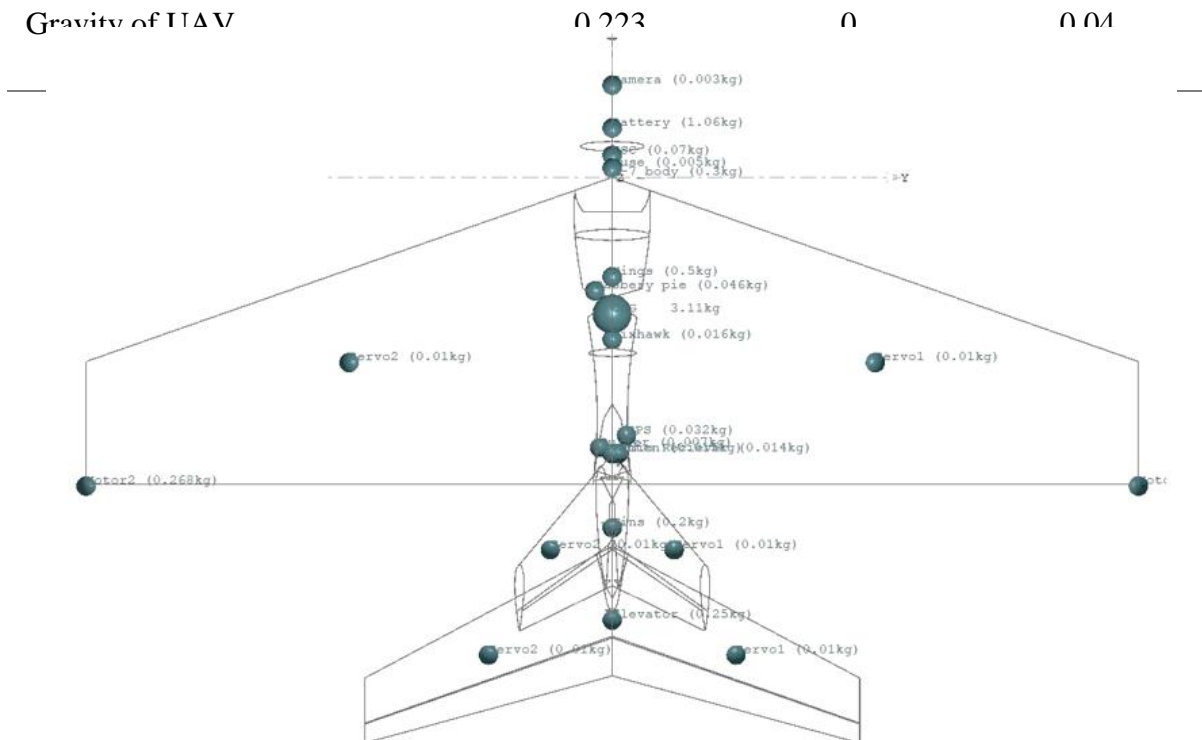


Figure 3.4 Weight Distribution

4. Autonomous Lockdown

What is Object Detection why we need it?

Object detection is a computer vision method to pinpoint objects of interest. It is crucial for making a UAV that can autonomously dogfight with other airplanes, it is frequently being used in other industries as well, and robotics surveillance quality checks for some big factories are all using object detection algorithms to automate the process and decrease the cost and increase the efficiency.

Methods of Object Detection

There are many ways to detect an object in an image or in a video stream, but if we were to classify we could divide them in three sub groups

1. Feature and color based object detection
2. Object Detection Using Deep Learning
3. Object Detection Using Machine Learning

Feature and Color Based Object Detection

These methods are way simpler and faster than their alternatives, but their use cases are limited and bounded by various factors such as color, size, background, and speed so they are not as robust and accurate and won't work on some types of aircraft but will work on other types thus this method hasn't been chosen to detect the aircraft. Figure 4.1 illustrates the color-based detection.

Figure 4.1 Color Based Object Detection



Object Detection Using Machine Learning

Machine learning is a reliable method to locate objects, they use coded algorithms by humans to detect certain types of similarities and detect those similarities, some methods of machine learning are as follows; Aggregate channel features (ACF), SVM classification using histograms of oriented gradient (HOG) features, The Viola-Jones algorithm for human face or upper body detection as you can see some of the algorithms such as the Viola-Jones algorithm is only for humans this is because that algorithm is making the machine search for humanoid features such as arms, noses, etc... this is the main difference of deep learning and machine learning in deep learning there is no algorithm to force the machine to look for certain features

machine find its own features on itself. And exactly for this reason, deep learning is computationally more expensive than machine learning. In figure 4.2 you can see an example of object detection with the ACF method



Figure 4.2 showing object detection with ACF method

Object Detection Using Deep Learning

Object detection with deep learning is the by far most favorite method of all object detection techniques it can be robust and fast, or it can be highly accurate and slow it can be manipulated if needed and pretty much can detect any object in any situation if enough training is done. But there is one big drawback to this method and that is; the sheer amount of computational power and a huge amount of training data that it needs to provide good quality detections. Deep learning algorithms work on neural networks, firstly the networks are trained classify the images, then objects detected in the classified images to provide high accuracy detections. Some of the popular deep learning-based object detectors are Yolo, Tensor Flow, and R-CNN these object detectors can learn to detect objects without having the set up the entire neural network.

There are two main approaches that can be followed; a custom network can be made to detect the features of the custom object which is to be detected, then an object detector can be trained on the custom network. This takes a lot of time but in the end, it produces remarkable results. The other approach is to take a pre-trained network and train a custom object detector on the network. The advantage of this approach is that it is faster to implement and requires less work and computational power and time.

There are two types of networks, two-stage, and single-stage networks, single-stage network identifies the image in a single stage while two-stage networks first identify and classifies the image to achieve higher accuracy at the cost of computational time and speed.

The Chosen Method to Detect UAV's in Dogfight

In a dogfight situation images move rapidly and get in and out of the visual sight often, this is why speed over accuracy is more valuable for our application. Other than the speed aspect

we also need a robust detector since the background of the objects and the objects themselves are in constant change. By taking these factors into consideration object detection via deep learning with a single-stage pre-trained network is chosen. The reason behind the choice to use a pre-trained network is that we don't have access to strong computational powers, and we wanted to decrease the time span for developing the detector. We chose the Yolo darknet network as our neural network and train a yolov2 detector to detect the objects of interest.

Tracking the Detected Object

An extra code has been written to track the movement of the object of interest, the code manages this by taking the difference of the centers on consecutive frames and dividing it by the time passed to get a linear and angular velocity of the object of interest relative to the observer (Camera). In figure 4.3 tracking code output can be seen.

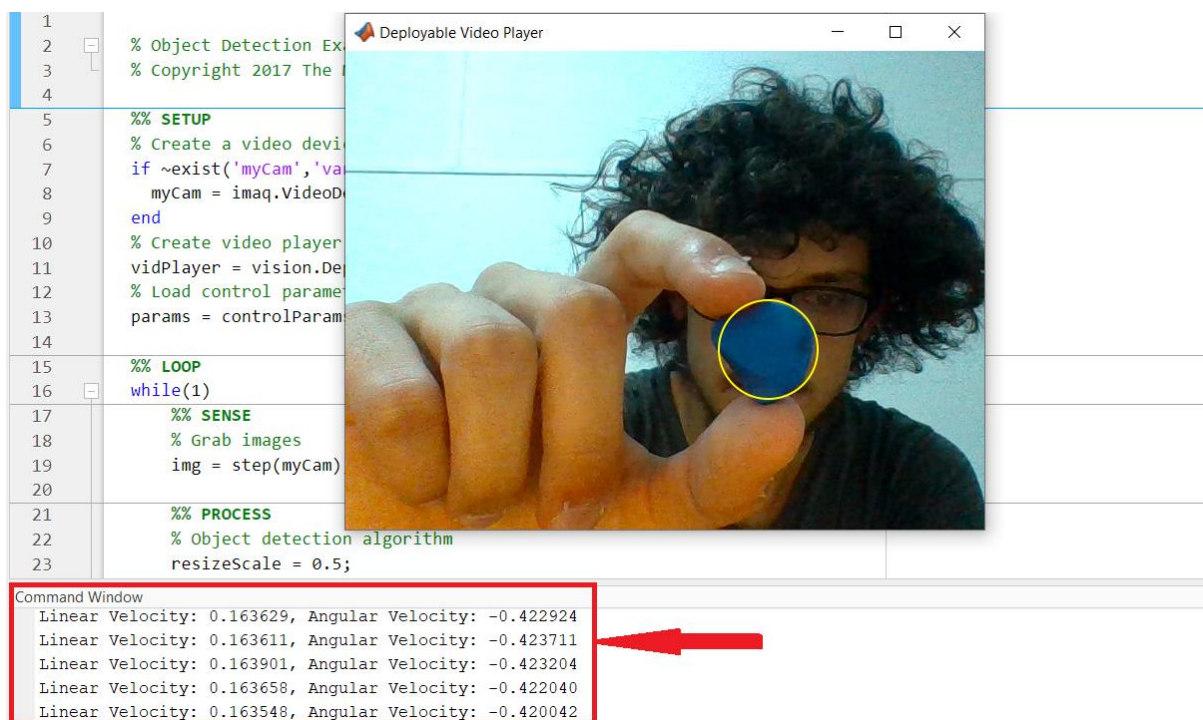


Figure 4.3 showing the output of the Tracking Algorithm

After learning the aircraft's relative speed and rotation, its data is sent to the autonomous flight code to update its speed and align itself with the aircraft being tracked. The general working scheme of the algorithm can be seen in figure 4.4.

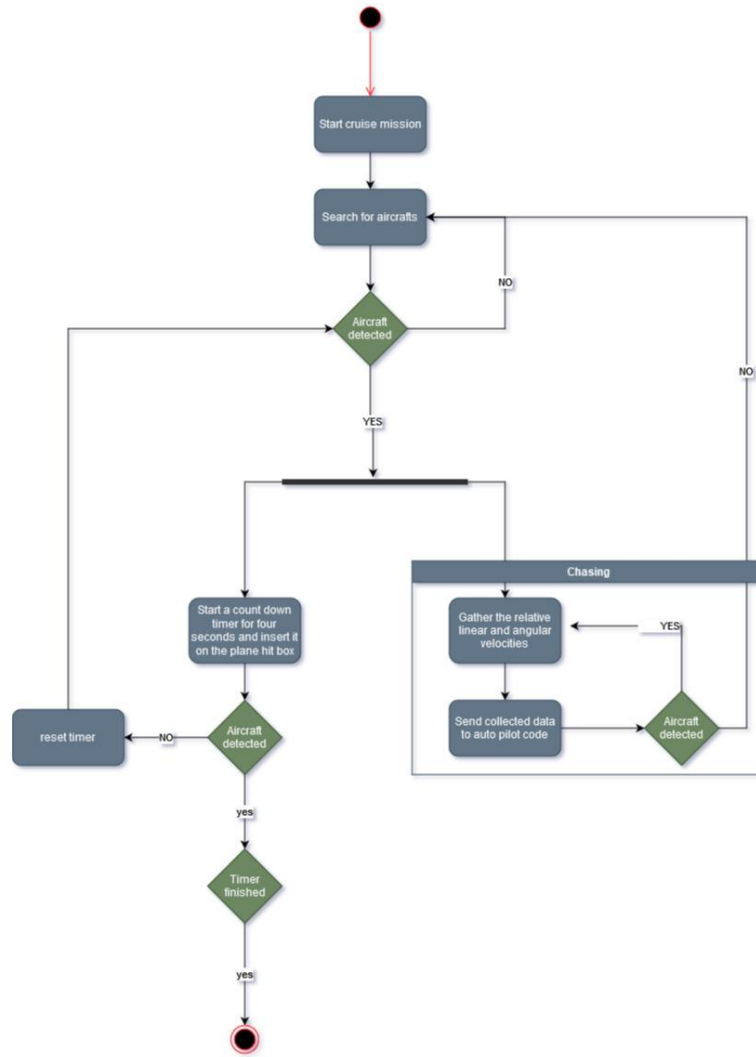


Figure 4.4 showing the flowchart of the algorithm

5. Communication

The Communication System is responsible for all the communication between the aircraft and the ground control station. A ground control station is a station where the aircraft can be controlled from the ground via an interface. During the mission the aircraft will collect some data, all those data should be transported, processed, and stored in real-time. In figure 5.1 the components of the Communication Systems and the communication protocols can be seen. By using these protocols different types of data can be transferred.

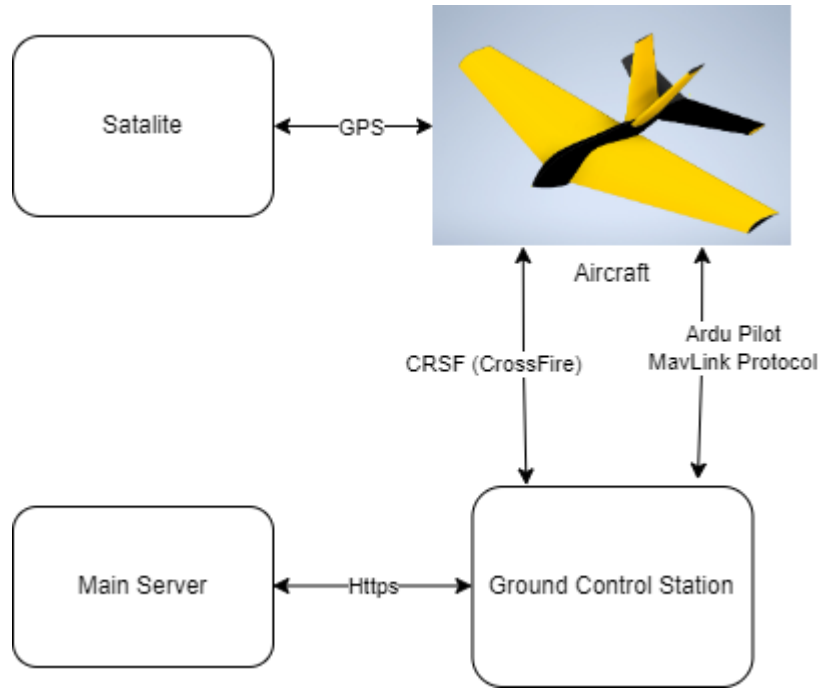


Figure 5.1 showing the components of Communication System and the Communication Protocols

Explanation of Telemetry Protocol

Telemetry is a next-generation communication technology that is used to send and receive data from various devices at high speed. Telemetry protocols are a method of commuting the information. The various companies have manufactured many different telemetry protocols. The compatibility of the protocols is essential in the communication of the components between the telemetry systems. Since we are using the ArduPilot as our autonomous flight code, we should use the protocol that supports the Ardupilot, which is nothing but Mavlink. Mavlink is a communication protocol that is developed by Ardupilot which is an open-source project. In fig 5.2 the Mavlink message protocol's frame can be seen.

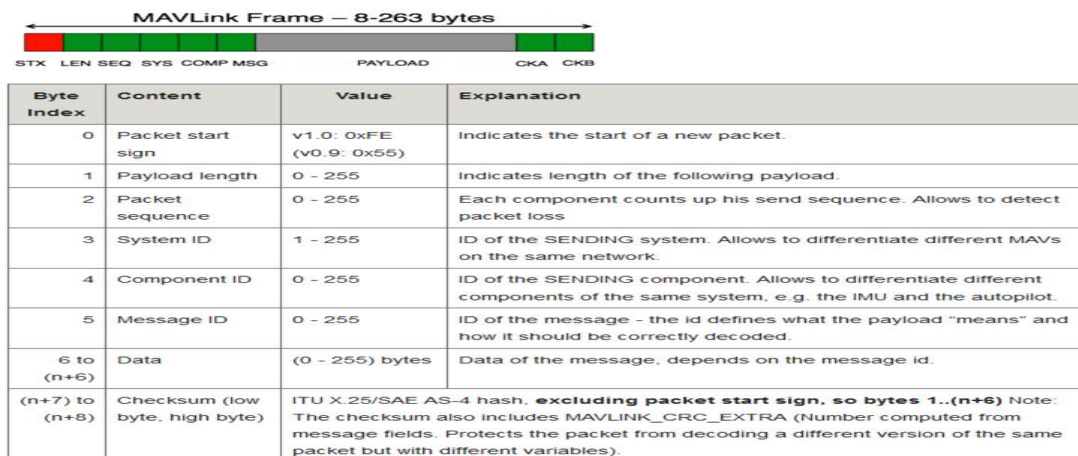


Figure 5.2 showing the Mavlink Message Protocols Frame

Telemetry communication is necessary for autonomous flight control when aircraft is in the air the operator needs information about the important parameters of the aircraft. To satisfy such needs telemetry communication is utilized. The telemetry transmitter will send the video

output of the camera as well as the longitude, altitude, and latitude values and the rotational and linear velocities, and many more. By collecting such information the state of the aircraft can be understood, and important decisions regarding the aircraft can be made.

Explanation of Radio Communication Protocol

RC protocols can be considered as a language talked between the components. It can be classified into two main categories Tx transmitter category and Rx the Receiver category. Most manufacturers have their own protocols and some of them even offer more than one protocol. It is important that the chosen radio receiver is compatible also known as using the same protocol with the transmitter. Our selected radio transmitter and receiver use CRSF (CrossFire) protocol. This protocol is developed by the company which manufactured the radio system. The main of this communication protocol is its fast update rate and its two-way communication capabilities. Radio communication is used for manual flight. In case the manual flight is necessary the pilot on the ground station will send input through a radio transmitter and the radio receiver will take the input and execute the maneuver.

Explanation of Https Communication

For HTTPS communication with the competition's main server, the server IP address will be taken from the competition authorities and be connected via the computer in the ground station. Then the necessary telemetry data that is gathered from the aircraft will be sent alongside the lockdown video to the main server. Also, the location of the other aircraft will be pulled from the system and used for the mission.

Explanation of Components

The components of the communication system are as follows

- 5.8 GHz 8 Channel RC805 FPV Receiver Module
- Computer
- Telemetry Transmitter 5.8 GHz 600Mw FPV Transmitter
- Radiolink R12DS 2.4GHz RC Receiver 12 Channels
- Radiolink AT9SG Pro 10 channel 2.4ghz

The Telemetry transmitter sends the data from aircraft to ground station .Some of the important properties of Telemetry transmitter can be seen in the table 5.1.

Telemetry Transmitter 5.8 GHz 600Mw FPV Transmitter	
Size	23.3*64.4mm
Brand	FPVDrone
Connectivity Technology	Wireless
Item Dimensions LxWxH	5 x 2.52 x 1.61 inches
Item Weight	0.09 Pounds
Table 5.1 showing some of the properties of Telemetry Transmitter	

The telemetry receiver takes the data that is sent from the transmitter and gave it to the computer. Table 5.2 shows some of the important properties of the telemetry receiver.

5.8 GHz 8 Channel RC805 FPV Receiver Module	
Output Frequency:	5.8Ghz
Receiving frequency:	5665-5945MHz
Channels:	8CH (Bands E)
Receiving sensitivity:	-90dBm
Input voltage:	8-12V
Supply current:	150mA
Dimension:	75x54x15mm
Weight:	130g

Table 5.2 showing some of the properties of Telemetry Receiver

Radio transmitter allows the aircraft controlled manually. The table 5.3 showing some of the important properties of the radio transmitter.

Radiolink AT9SG Pro 10 channel 2.4ghz	
Dimensions:	183x100x193mm
Weight:	0,880 gr
Frequency:	2.4GHz
Modulation mod:	QPSK
Band width:	5.0MHz
Spectrum Mod:	DSSS&FHSS/CRSF
ACPR	: >38dbm
Connection Power:	DSSS & FHSS <100mW(20dbm)
Work Current:	DSSS&FHSS < 90mA @ 12V
Work Voltage:	7.4~18.0V
Control Span:	DSSS&FHSS - 4000m
Signal Output:	PWM/SBUS/PPM/CRSF
Compatible Receivers:	12CH - R12DSM, R12DS 10CH- R9DS(Std), R6DS, R6DSM

Table 5.3 showing some of the properties of Radio Transmitter

Radio receiver is the thing that takes the transmitters input and turns it into output. The table 5.4 showing some of the important properties of the radio receiver.

Radiolink R12DS 2.4GHz RC Receiver 12 Channels	
Color	Black
Item Dimensions LxWxH	1.97 x 1.24 x 0.57 inches
Brand	Radiolink
Item Weight	0.49 Ounces
Item Package Quantity	1

Table 5.4 showing some of the properties of Radio Receiver

The Computer is the main part of the ground control station, the interface which is going to control to aircraft will run on the computer. Also, the communication between the main server and the ground station will run solely on the computer as well. With these being said the interface does not require high ram nor the GPU so any computer would work just fine, but it is better if a strong computer is chosen, we have chosen our own personal computers to decrease the price of the project.

6. User Interface Design

User Interface Design

The Mission Planner is a robust and powerful program that provides an interface for autopilots not just for aircraft, but also for radio-controlled land vehicles, boats, submarines, and even more. The team is interested in the auto plane part of Mission Planner only, and the Mission Planner has been chosen program as our user interface. The following reasons have been considered when taking this decision;

- It's compatibility with ArduPilot autopilot code
- It's ease in using and learning
- It's ability to be easily modified via python scripts
- Its position as a well-documented and open sourced program (free)
- It's capability to support telemetry operations
- Its provision of enabling geographical map data and visualizing the environment in 2D

Introduction to the Mission Planner

Mission Planner provides a flight data screen to users so that they can see and interpret the related information about their aircraft. In figure 6.1 flight data screen can be seen. In the figure, there are three main parts that provide visual data about the aircraft. The first screen is a geographical map that shows the geographical position of the aircraft, on the same screen the path of the aircraft can be seen as well as the altitude, longitude, and latitude. Some other information can be gathered from the map as well. The second screen can be seen in fig 6.2.



Figure 6.1 showing the Flight Data screen of Mission Planner

Figure 6.2 is the HUD (heads up display) it provides important information about the aircraft. And that information can be obtained from table 6.1.

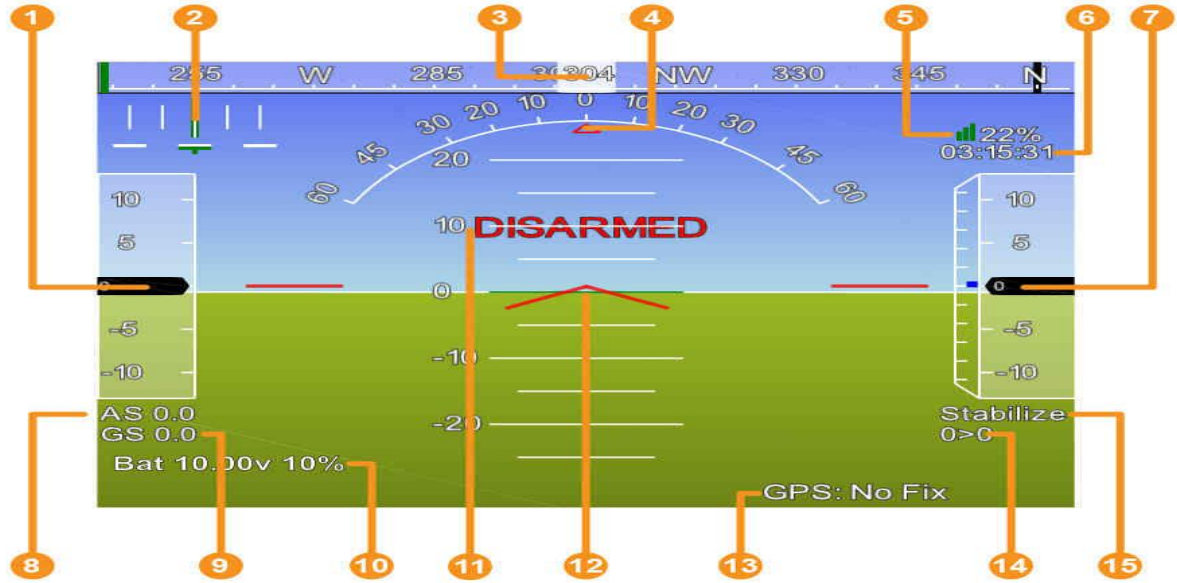


Figure 6.2 showing Heads-Up Display of Mission Planner

HUD Screen Data	
1.	Air speed (Ground speed if no airspeed sensor is fitted)
2.	Cross track error and turn rate (T)
3.	Heading direction
4.	Bank angle
5.	Telemetry connection link quality (averaged percentage of good packets)
6.	GPS time
7.	Altitude (blue bar is rate of climb)
8.	Air speed
9.	Ground speed
10.	Battery status
11.	Artificial Horizon
12.	Aircraft Attitude
13.	GPS Status
14.	Distance to Waypoint > Current Waypoint Number
15.	Current Flight Mode

Table 6.1 showing Heads-Up Display's Data

Regarding the Lockdown rectangle, the plan was to acquire the image via camera, process it via Raspberry pi, and send it to the ground station via telemetry transmitter, but since we had neither the camera nor the telemetry receiver and the transmitter and also image processing computer. We couldn't actually gather the image to put into the HUD. So instead we used our computer's webcam to gather the image and put the lockdown triangle in it. And then we put the image on the interface. In figure 6.3 you can see the results.

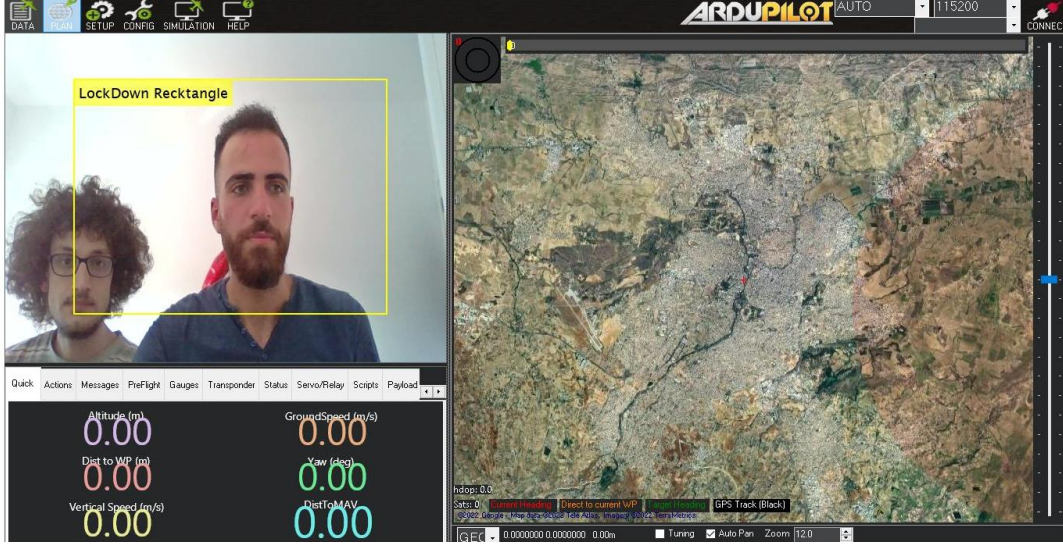
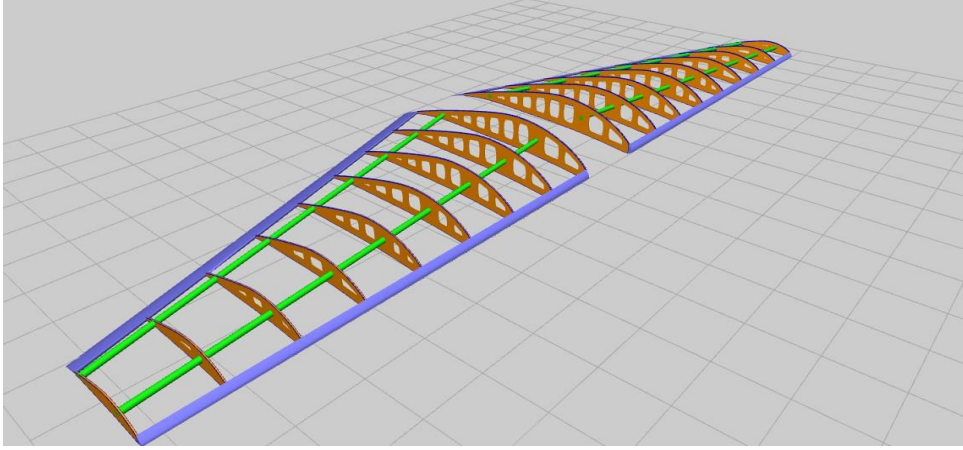


Figure 6.3 showing Head-Up Display of Mission Planner

7. AIRCRAFT INTEGRATION

7.1 Structural Integration

The wing design, which is one of the components of the aircraft, was drawn in detail thanks to Wing Helper. In this section, the wing slats that we will make with balsa wood are designed to be lighter by being emptied and can be adjusted according to the spar from the inside. The spars passing from the ribs are selected from carbon fiber to provide strength and stability. In addition, where the spar's holes has been calculated and visualized in the Wing Assistant. The upper trim material of the wing is made of carbon fiber. In this way, it is ensured that it is both flexible and durable. After the shapes of the ribs were determined, they were drawn with Autodesk Inventor Professional and analyzed with Fusion 360 for analysis. The figure shown in Figure 7.1 easily illustrates the ribs and spars configuration.



Figure

7.1

showing the inside of the wing drawn with the help of Wing Helper

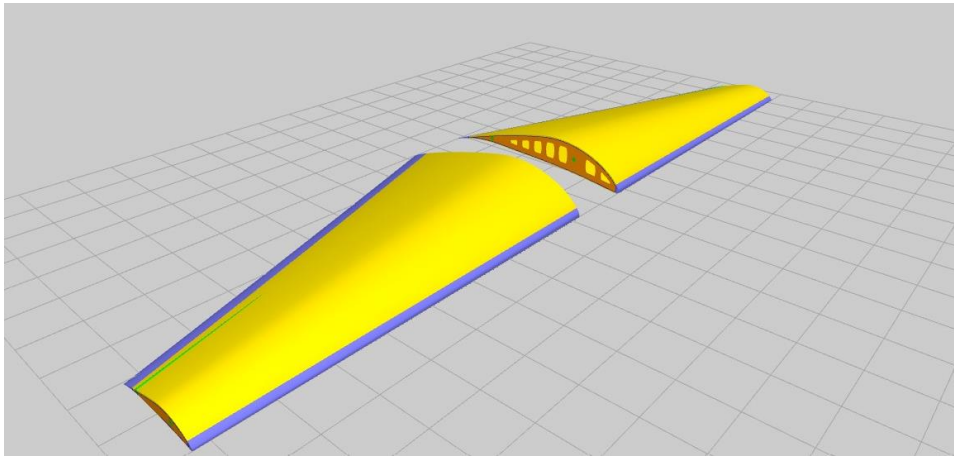


Figure 7.2 showing the surface of the wing drawn with the help of Wing Helper

7.2 Mechanical Integration

The engines of the aircraft will be mounted on the wing tips. This will be done by first making an engine mount on the wingtip. The engine mounts can be seen in figure 8.1.

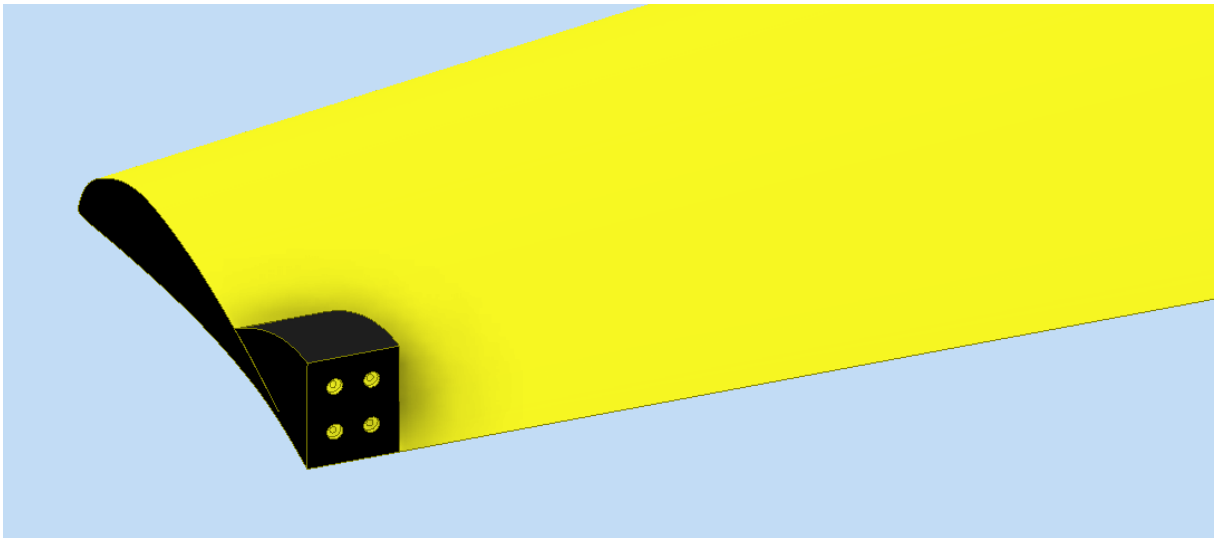


Figure 7.1 showing the Engine Mounts on the wingtip without the engine

The engine will be mounted on the holes on the engine mount via screws. Since our team's selected engine is an out-runner first the engine will be mounted and screwed on the secondary piece then the second piece will be screwed to the engine mount which can be seen in figure 8.1. In figure 8.2 the secondary piece can be seen.



Figure 7.2 showing the engine mount



Figure 7.3 Showing the holes at the bottom of the engine

The holes at the bottom of the engine which will be screwed at the secondary piece can be seen in figure 8.3 as well.

The antenna should be away from the camera. Thus antenna is going to be mounted on the tail of the aircraft. Also in order not to create an unbalanced drag and cause a constant drag on the aircraft it is located in the middle of the aircraft in figure 8.4 you can see the position of the antenna..

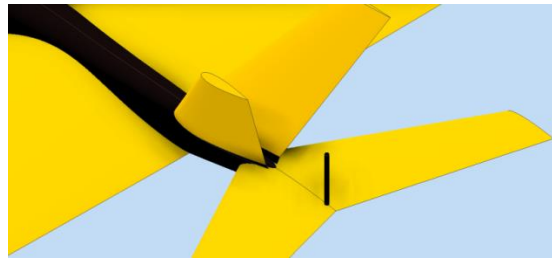


Figure 7.4 showing the position of the Antenna

The antenna is going to be mounted inside the fuselage, and inside the fuselage, there is going to be a mounting layer to put all the electronics in. the Raspberry pi is also going to be mounted inside the fuselage. While the plane is moving and making sharp turns in order not to prevent the movement of the inside electronics all the electronic parts will be mounted on the plane via straps and screws. Since the aircraft isn't built yet and the electronics haven't been purchased we can show an example view of how the mechanical integration is made in figure 8.5 an example figure by the 'Flight coach' Website can be seen. [10]



Figure 7.5 showing an example view of how the inside of the fuselage will look like and how the components will be placed and mounted

7.3 Electronic Integration

In the electronic integration part of the project, a power distribution board (PDB) was first created and the main power source, the lipo battery, was connected to it. Then power was transmitted from the PDB to the motors with the help of motor drivers (ESC). In addition, power modules were used to set the appropriate voltage and current for the Pixhawk and raspberry pi used for autonomous controls, and they were connected between the boards and the PDB.

In addition, a camera module was connected to Raspberry Pi for object detection, and a GPS module was connected to Pixhawk to determine location, telemetry for communication, ESCs to drive the motors, and a receiver to manually control the aircraft when necessary.

In the figure 7.6 the electronic integration demonstration can be seen.

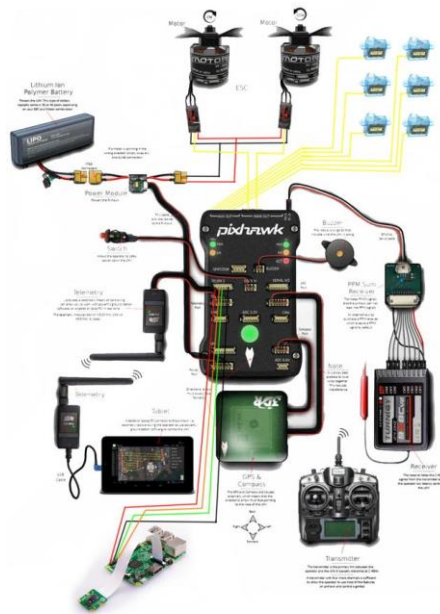


Figure 7.6 showing the electronic integration and how it is going to be done

8. TEST VE SIMULATION

8.1 Subsystem Tests

8.1.1 Lockdown Test of the Deep learning algorithm

The testing of the trained algorithm to understand whether or not a successful detection can be made is necessary. However the testing should be done with different kind of pictures than the ones used in the training of the algorithm. This precaution makes the test result more reliable and trustworthy. In the figure 9.1 it can be seen a successfully detected aircraft.



Figure 8.1 showing the detected UAV on the picture

Another picture can be seen in figure 8.2

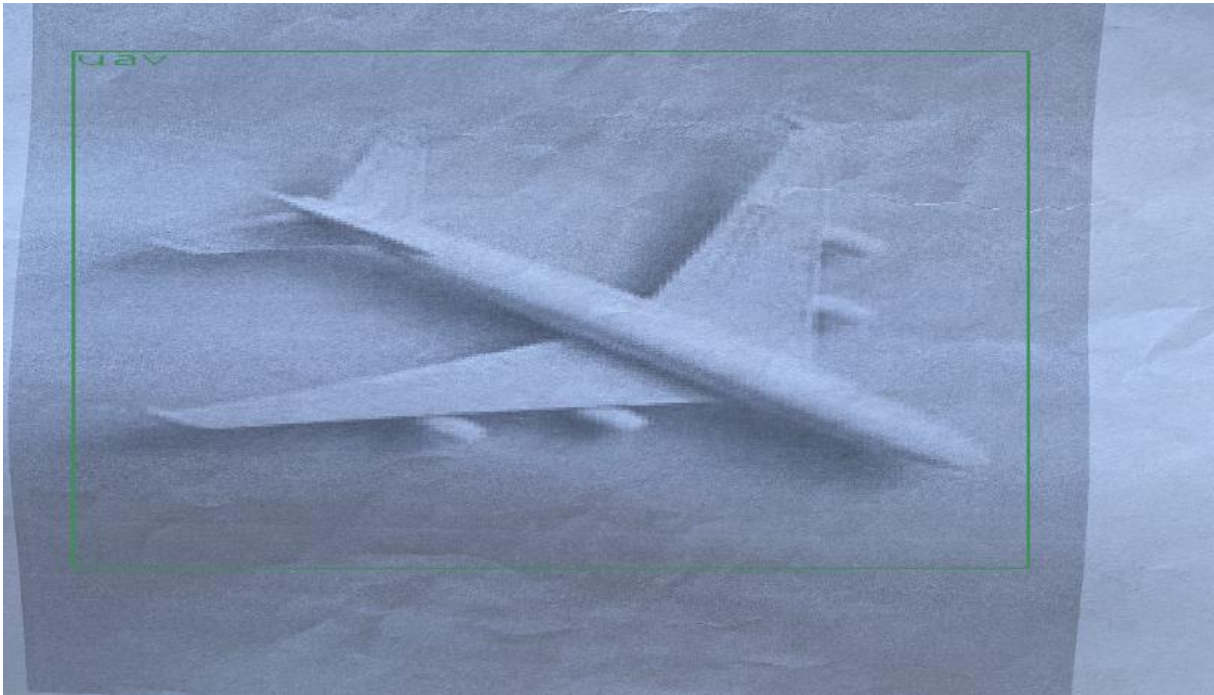


Figure 8.2 Showing the detected uav in the another picture

Another Picture can be seen in figure 8.3



Figure 8.3 showing the detected uav on another picture

This test tried on multiple pictures and the results were great all the pictures except one picture are detected and the one which the code failed to detect was a very low-quality picture the quality was even worse than 144p and thus the detector failed to detect it. To sum up, after this test we can say that we have an accurate and fast detector to be used in the UAV to chase the aircraft.

8.1.2 Strength Analysis of Composite Wing and Computational Fluid Dynamics of UAV

As a result of the stress analysis test, airfoil analysis was performed. Balsa wood has been chosen as the airfoil material for this test. In addition, a total of 3 spars, 1 main spar and 2 side spars, were used in the wing. Carbon fiber epoxy is used as both the wing surface and the Spar material. The main purpose of this test is to find the deformation of the load on the wing and the safety factor of the wing. As a result of the calculations, the load on the wing was found to be 5.042 kg/m^2 . Area of the wings is equal to 0.595 m^2 . When the load on the wing is multiplied by the wing area, the load on the wing is calculated as 3.022679 kg . However, in order to obtain a more realistic result in the analysis, the load falling on the wing was calculated as 20.04 kg and the analysis was made according to this load. Stress analysis test performed with the maximum load on the wing resulted as 21.58 mm wing tip deformation. Considering the flexibility of the wing, this deformation does not have a significant effect on the wing. Because as a result of another analysis, Factory of Safety was above 15 for almost all wing, including the wing tip. Therefore, the minimum factory safety was obtained as 2,956. In the light of this information, it has been proven that our wing can easily carry a load of 20 kg .

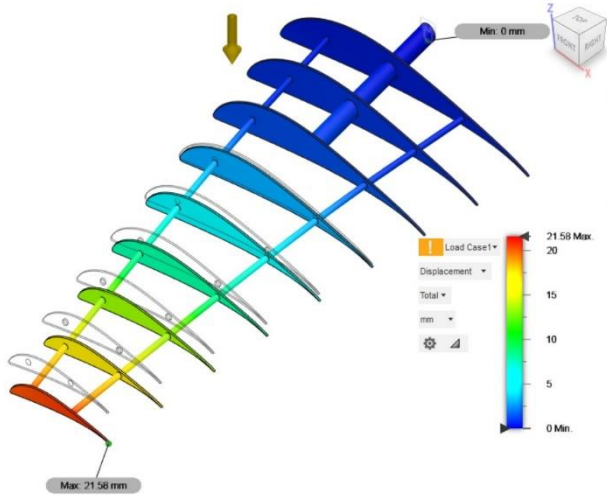


Figure 8.4 the Deformation distribution

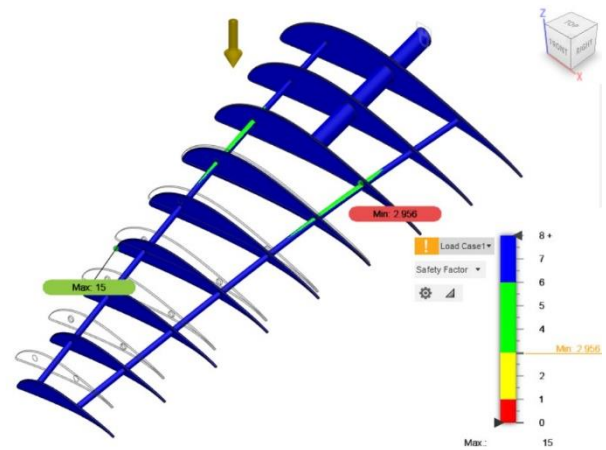


Figure 8.5 the Factor of Safety

In Figure 8.4, the deformation distribution due to the loads on the wing is shown in colors from minimum to maximum. In Figure 8.5, the factor of safety distribution is indicated due to the load on the wing.

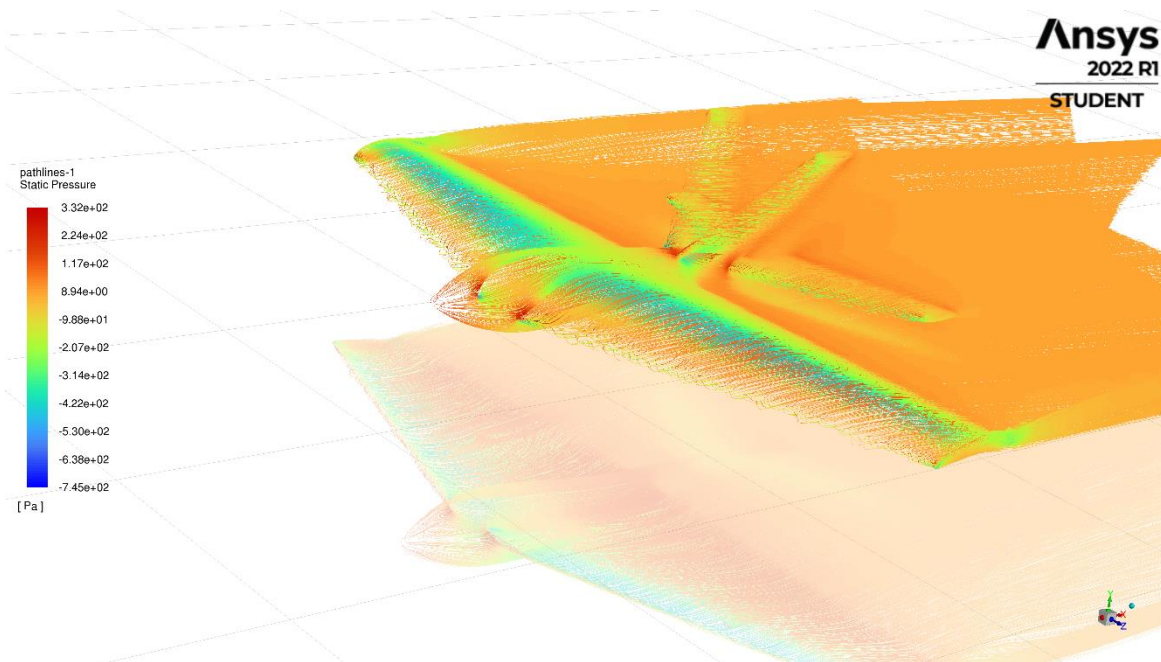


Figure 8.6: Static Pressure Distribution throughout UAV

This figure 8.6 shows the static pressure distribution over the UAV. In the figure 8.6, while the maximum value is seen at the point where the wing and the fuselage intersect at front, and the lowest values are seen on the upper surface of the wings.

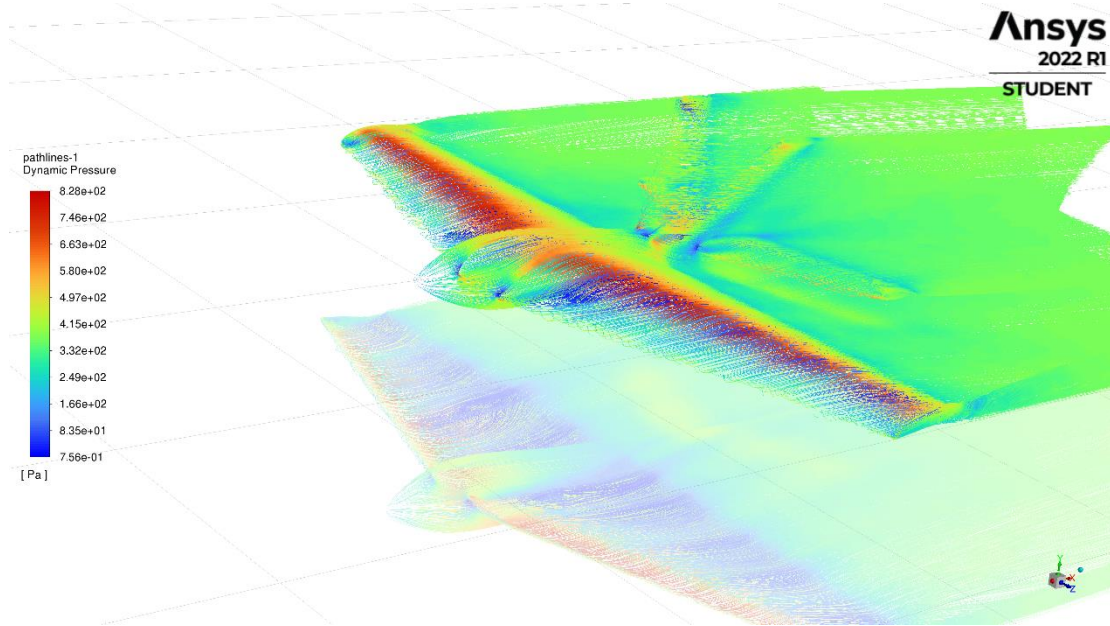


Figure 8.7: Dynamic Pressure Distribution throughout UAV

This figure 8.7 shows the dynamic pressure distribution over the UAV. In the figure, while the maximum value is seen at the upper wing surface, and the lowest values are seen at the lower surface of UAV.

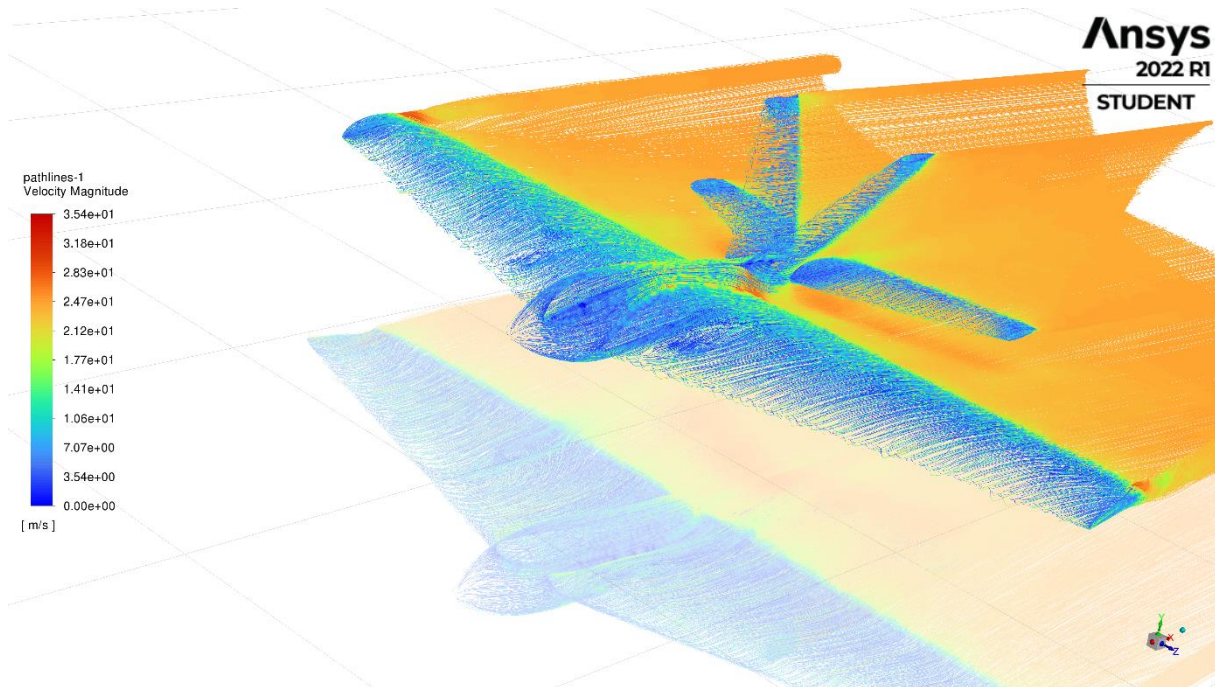
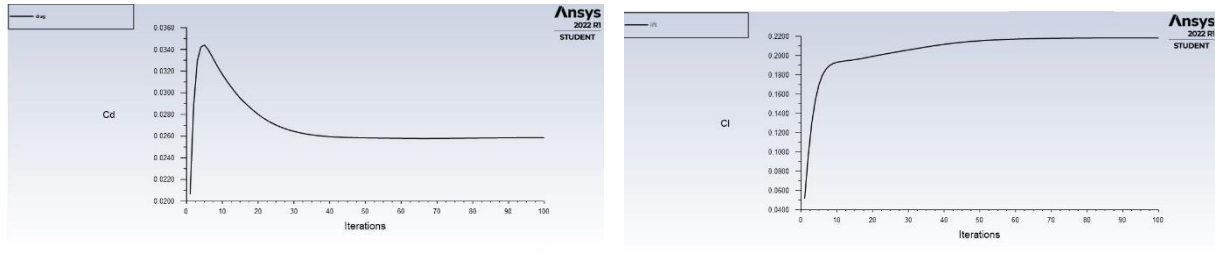


Figure 8.8: Velocity Magnitude Distribution of UAV

This figure 8.8 indicates the velocity magnitude distribution on the UAV while traveling at a cruise speed of 25 m/s with a zero-degree angle of attack. The highest velocity magnitude value is obtained as 35.4 m/s at the behind the wing.



(a)

(b)

Figure 8.9 a, and b: Coefficient of Lift and Drag

Figure 8.9 a shows the distribution of drag coefficient change due to iterations. As a result of the iterations, the drag coefficient, C_d , was converged to 0.02586. In Figure 8.9 b, the distribution of lift coefficient changes due to iterations. As a result of the iterations, the lift coefficient, C_l , was converged to 0.21841. These results are almost the same with the values found when calculating the drag coefficient.

8.1.3 Thrust Test of the RC Engines

The thrust test is performed by using a kitchen balance that can measure weight up to 5 [kg] with ± 100 [g] accuracy, the engine, propeller, and ESC as well as the battery and the motor control unit. The figure 8.10 you can see the experimental setup.

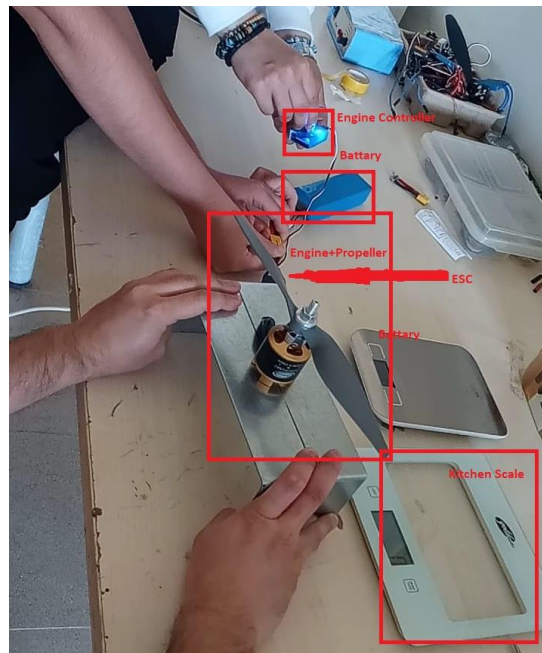


Figure 8.10 showing the Experimental Set-up

The battery was a 3-cell LiPo battery which had a lower cell and thus lower voltage value than what we wanted for our engine. This mainly happened because the team couldn't take the battery for the aircraft so they have to borrow a battery from a fellow student. The out-runner engine is mounted on sheet metal and the sheet metal is placed on the kitchen scale. Then using the motor control unit the engine's power of the engine is adjusted. Also, it is worth noting that, in this set up in order to measure the thrust of the engine should apply backward thrust that why the propeller is mounted inverse. We also tried changing the current flow to change the direction of the thrust and that worked but not as well as the inversely placed propeller. In figure 9.11 you can see the thrust test while the test is still going on.



Figure 8.11 showing the Thrust test on process

We also wanted to measure the current that the engine is taking at the moment so we changed the experiment set up after that experiment was over. We added a current measurement device called Digital pens ampere-meter which can measure ampere even through the plastic surface of the cable. In figure 9.12 the updated experiment can be seen.



Figure 8.12 showing the Updated Experiment

The results of the experiment was the followings,

Max Thrust of the engine	0.6 [Kgf] \cong 5.9 [N]
Burst Current ()	4.5 [A]
Continuous current ()	0.55 [A]

Table 8.1 showing the Experiment Result

As can be seen in table 8.1 maximum thrust of the engine is 6 [N], the burst current of the ESC is 4.5 [A] and the continuous current is 0.55 [A]. which is very shocking since there

are other thrust tests of the same engine model on the internet that get values like 1.5 [kgf] of thrust from a single-engine. Also, an engine of this size 6 [N] is a very small thrust force, this seems like an experimental error and it could happen because of any of these two factors; poor measuring devices and a 3s battery may not provide enough voltage. To have a better idea about this engine's power this video from 'MrMotor' [1] YouTube channel can be watched in his video he uses a similar engine to ours with proper setup and a 4s battery and gets 1.2 [kgf] of thrust. In figure 9.13 the result thrust test of the 'MrMotor' youtube channel can be seen.



Figure 8.13 showing the result of the thrust test made by 'MrMotor' YouTube Channel

Nevertheless if our engines real capacity is 0.6 [kgf] and there is no experimental error then our aircraft still going to fly with the speeds up to 20-25 [m/s] but not 30-35 [m/s]. In both cases this test proves that the engines that we choose are more than capable of providing enough thrust for our aircraft.

8.2 Flight Test and Control List

8.2.1 Flight Test

Unfortunately, the UAV couldn't be built by the time this report is written due to financial issues. The sponsorship deals couldn't be closed and thus the necessary amount of money could not be collected. And yet the team managed to save a small amount of money that is only enough to buy the RC engines and the ESCs and Propellers. The rest of the components and building materials will be received after the submission of the Critical Design report.

8.2.2 Flight Control List

Before flight, it is wise to make sure that your system will work properly. So a pre-flight check is necessary. In this list, the following steps must be checked.

- Control Surface Check
- Aircraft's Structure Check
- Check the angle of the wings and the tails
- Check the Communication devices and connection stability
- Check the battery Voltage (whether charged or not)
- Check the transmitter's Power
- Check the physical connections of the components (screws, hinges etc...)
- Check the propeller
- Check the Motor

- Check the Servos
- Check the Center of the Gravity
- Check for people around
- Check for building around
- Check for other flying objects around (Other aircraft, birds etc...)

This checklist enables the team to avoid accidents and unwanted situations. Before and after every flight these steps must be checked and make sure every one of them working properly. If not it should be fixed and until its fixed aircraft should not perform any flight mission.

3. Safety

The current values of all electronic equipment and propulsion system used in the UAV have been calculated in order to fly at maximum power during cruise flight. As a result of these calculations, an ESC, that can handle 15% more current, has been selected. At the same time, a fuse button suitable for the main power output has been added. Pressing this fuse button in an emergency will shut down the entire system. Carbon fiber, bolts, silicon, and tape will be used to strengthen all moving parts of the UAV, especially the control surfaces. The load that the servos can handle has been calculated analytically and selected accordingly. It is planned to hold the servo motors with plastic clips and silicone in such a way that they remain without moving in the wings. When the maximum take-off weight of the UAV has been calculated, according to stress analyses, the minimum safety factor seen on the wing has been found to be 3. As a result of this analysis, it is seen that the wings do not create a security weakness. A pre-flight safety list has been created (8.2.2). Thanks to this security list, it is aimed to minimize the security weakness by following the pre-flight and post-flight control steps. It is planned to minimize the risk of current leakage by covering the electronic circuit elements and cables used in the UAV with insulating material. It has been taken into account that the subsystems that are heated during operation do not come into contact with each other. It is planned to be attached to the battery holder with screws so that our batteries do not move. This will reduce vibration. It is planned to protect our batteries with lipo protector when they are removed from the UAV for charging. The propeller is fixed to the engine with the proper mounting method. It is planned to fix the wing and motor to the body by using metal screws and fibber nuts, and vibration-related problems are prevented. During the construction of the UAV and during the flight return, safety clothing will be used to protect the hands, eyes, and head areas due to reasons that may cause an accident. Some of these outfits require wearing a helmet, fire and cut-resistant gloves, and goggles.

4. REFERENCES

- [1] “Freewing 3536 800KV brushless motor thrust test with 11X6L propeller and 3S,4S Lipo,” *YouTube*, 07-Sep-2021. [Online]. Available: https://www.youtube.com/watch?v=DWRCoYHuugc&ab_channel=MrMotor. [Accessed: 31-May-2022].
- [2] “Autodesk empowers innovators everywhere to make the new possible,” *Autodesk*, 29-Apr-2022. [Online]. Available: <https://www.autodesk.com/>. [Accessed: 30-May-2022].
- [3] “General description Xflr5,” *XFLR5*. [Online]. Available: <http://www.xflr5.tech/xflr5.htm>. [Accessed: 30-May-2022].
- [4] “Makers of Matlab and simulink,” *MathWorks*. [Online]. Available: <https://www.mathworks.com/>. [Accessed: 31-May-2022].
- [5] “Welcome to Python.org,” *Python.org*. [Online]. Available: <https://www.python.org/>. [Accessed: 31-May-2022].
- [6] DEMIRCAN, Alpay. *Aerodynamic and structural design and analysis of an electric powered mini UAV*. 2016. Master's Thesis. Middle East Technical University.
- [7] “Ansys | Engineering Simulation Software.” [Online]. Available: <https://www.ansys.com/>. [Accessed: 31-May-2022].
- [8] ArduPilot, “Ardupilot,” *ArduPilot.org*. [Online]. Available: <https://ardupilot.org/>. [Accessed: 31-May-2022].
- [9] “Draw io,” *Draw.io*. [Online]. Available: <https://www.draw.io/connect/office365/index.html>. [Accessed: 31-May-2022].
- [10] “Capturing your first log file,” *Flight Coach*, 15-Feb-2021. [Online]. Available: <https://www.flightcoach.org/installation-inside-model/>. [Accessed: 31-May-2022].